Geosci. Model Dev. Discuss., 6, 2325–2368, 2013
www.geosci-model-dev-discuss.net/6/2325/2013/
doi:10.5194/gmdd-6-2325-2013

Geoscientific Model Development Discussions
Open Access

The Simulator of the Timing and Magnitude of Pollen Season (STaMPS) model: a pollen production model for regional emission and transport modeling

T. R. Duhl[1], R. Zhang[2], A. Guenther[1], S. H. Chung[2], M. T. Salam[3], J. M. House[4], R. C. Flagan[4], E. L. Avol[3], F. D. Gilliland[3], B. K. Lamb[2], T. M. VanReken[2], Y. Zhang[5], and E. Salathé[6]

[1]National Center for Atmospheric Research, Atmospheric Chemistry Division, Boulder, CO, USA
[2]Labortatory for Atmospheric Research, Department of Civil and Environmental Engineering, Washington State University, Pullman, WA, USA
[3]University of Southern California, Los Angeles, CA, USA
[4]Department of Chemical Engineering, California Institute of Technology, Pasadena, CA, USA
[5]National Center for Atmospheric Research, Research Applications Laboratory, Boulder, CO, USA
[6]Climate Science and Policy, Science and Technology Program, University of Washington, Bothell, WA, USA

Received: 30 January 2013 – Accepted: 13 March 2013 – Published: 4 April 2013

Correspondence to: A. Guenther (guenther@ucar.edu)

Published by Copernicus Publications on behalf of the European Geosciences Union.

Abstract

A pollen model that simulates the timing and production of wind-dispersed allergenic pollen by terrestrial, temperate vegetation has been developed to quantify how pollen occurrence may be affected by climate change and to investigate how pollen can interact with anthropogenic pollutants to affect human health. The Simulator of the Timing and Magnitude of Pollen Season (STaMPS) model is driven by local meteorological conditions and is designed to be sensitive to climate shifts, as well as flexible with respect to the vegetation species and plant functional types (trees, grasses, etc.) represented and the climate zones simulated. The initial focus for the model is the simulation of the pollen emission potential of important allergenic tree and grass species that typically flower between March–June in Southern California (S. CA), which is characterized by moderate Mediterranean and oceanic climate zones as well as regions of arid desert and arid steppe. Vegetation cover and species composition data are obtained from numerous datasets and a database of allergenic vegetation species, their pollen production potential and relative allergenicities has been developed. For the selected allergenic species and spring-early summer simulation period, temperature is the main driver controlling the timing of pollen release, while precipitation (and temperature, for some species) controls the magnitude of pollen produced. The model provides species-specific pollen potential maps for each day of the simulation period; these are then used by a pollen transport model to simulate ambient pollen concentrations as described in a companion paper (Zhang et al., 2013a), which also presents model evaluation results for the S. CA model domain. The STaMPS model was also used to quantify the possible impact of climate change on pollen season under the IPCC SRES A1B scenario as simulated by the ECHAM5 global climate model. Current (1995–2004) and future (2045–2054) meteorological conditions downscaled using the Weather Research and Forecasting (WRF) model were used to drive STaMPS and generate estimates of the relative magnitude and timing of pollen season for important allergenic tree and grass species that bloom from March through June in a larger domain that covers all of CA

GMDD
6, 2325–2368, 2013

and Nevada. Differences in the simulated timing and magnitude of pollen season for the selected allergenic species under current and future climate scenarios are presented. The results suggest that across all of the simulated species, pollen season starts an average of 5–6 days earlier under predicted future climatic conditions with an associated average annual domain-wide temperature increase of about 1 °C compared to simulated current conditions. Differences in the amount of pollen produced under the two scenarios vary by species and are affected by the selected simulation period (1 March–30 June). Uncertainties associated with the STaMPS model and future model development plans are also discussed.

1 Introduction

Allergic airway diseases are a major contributor to chronic disease in the US: up to 30 % of adults and 40 % of children suffer from hay fever in the US (Wallace et al., 2008), which is estimated to cause 3.5 million lost workdays in adults and 2 million missed schooldays among US children annually (Nathan, 2007). Asthma, a condition with allergic components in up to half of patients (Greenwood, 2011), afflicts over 8 % of the total US population (Akinbami et al., 2011) and is becoming increasingly prevalent (CDCP, 2011). In 2007, the total cost of asthma, including both direct (e.g. hospital stays) and indirect costs (such as lost productivity), was estimated at 56 billion US$ in the US alone (CDCP, 2011).

Various air pollutants can act as adjuvants to allergenic pollen, increasing the frequency and/or severity of allergic airway diseases (Gilmour et al., 2006), thus it is important to be able to predict the timing of pollen season relative to times of peak pollution, such as ozone season. For many plant species, flowering times and other phenological events occur earlier each year than in past decades as the climate warms (e.g. Fitter and Fitter, 2002; Frenguelli et al., 2002); atmospheric pollen burdens also appear to be increasing (Frei, 1998). Considering the high economic and quality-of-life costs associated with allergic airway diseases, and the uncertainties surrounding

GMDD
6, 2325–2368, 2013

future pollen episodes, the ability to predict the timing and magnitude of pollen season under changing climatic regimes is paramount.

Here we present the Simulator of the Timing and Magnitude of Pollen Season (STaMPS) model, a module of the Model of Emissions of Gases and Aerosols from Nature (MEGAN; Guenther et al., 2006, 2012). STaMPS simulates the pollen production capacity and the timing of pollen season for a range of anemophilous (wind-dispersed) allergenic plant species, and can be driven either by local observed temperature and precipitation conditions or by predictions provided by models such as the Weather Research and Forecasting (WRF) model (Skamarock et al., 2008). The STaMPS model is flexible in terms of the plant species and plant growth forms (e.g. trees, grasses, etc.) that can be included and in its potential spatial extent from local scale (meters to kilometers) to regional scale (100's to 1000's of km). Modeled relationships between meteorological variables and the timing/magnitude of pollen season for selected species were derived from the literature as well as available observational data. STaMPS simulations provide genus-specific pollen potential maps for each day of a chosen simulation period; these can then be used as inputs to a pollen transport model that generates airborne pollen concentration estimates, as fully described in a companion paper (Zhang et al., 2013a). After describing the model, results are reported for a 1 March–30 June simulation period in a domain centered over California and Nevada, in which STaMPS was run using simulated average daily temperature and precipitation for current (taken as average daily values for 1995–2004) and future (2045–2054) simulation periods. Uncertainties and limitations associated with the STaMPS model, as well as plans for future module development are presented.

2 Methods

For the present study, six tree genera, (*Betula*, *Juglans*, *Morus*, *Olea*, *Platanus* and *Quercus*) and one grass genus (*Bromus*) were selected for simulation (Table 1). These represent more than 30 allergenic species that typically bloom between March–June

GMDD
6, 2325–2368, 2013

within a S. CA study domain (Fig. 1, lower right). The selection of species to be included in the initial simulations was made using pollen count data for Pasadena, CA along with the expertise of co-authors who have been studying local pollen in S. CA for a number of years.

The environmental drivers controlling the onset and magnitude of pollen season must be known to simulate how much pollen is produced in a given season and when it will become available for release into the atmosphere. Temperature is the most important predictor of the timing of bud-burst and flowering in winter- and spring-blooming temperate tree species, while in species that bloom during other times, photoperiod is also an important determinant of flowering time (Frenguelli and Bricchi, 1998; García-Mozo et al., 2002). Flowering in temperate grass species is generally determined by both photoperiod and temperature, although in Mediterranean grasses, the photoperiod requirement is low (Heide, 1994). The magnitude of pollen produced in a given season is mainly a function of precipitation in some tree and grass species, and of both temperature and precipitation in others (Fairley and Batchelder, 1986; Gleichsner and Appleby, 1996).

Although flowering across the various plant functional types (PFTs; e.g. trees, grasses) may be controlled by the same variables, the relationships between these variables differ between PFTs, as do the timescales over which they operate. Therefore, STaMPS is organized by separate modules that compute the timing and magnitude of pollen season for early spring to late summer-flowering tree and grass PFTs within a given gridded model domain, as described in the following sections.

2.1 Predicting the onset of pollen season for trees

2.1.1 The thermal time approach

To predict the timing of anthesis in trees that flower during spring to early summer (when temperature is the main driver controlling flowering), the widely used thermal time model of Snyder (1985) is applied. The thermal time approach initiates pollen

GMDD
6, 2325–2368, 2013

release after a prescribed, species-specific threshold of heat-accumulation units, or Growing Degree Days (GDD), is achieved. The daily contribution to GDD accumulation above a prescribed base temperature (T_B, a species-specific temperature below which growth ceases) is calculated as:

$$\mathrm{GDD} = \begin{cases} 0, & \text{for } T_{max} < T_B \\ 1/\pi[(T_{avg} - T_B)(\pi/2 - \theta) + R \cdot \cos(\theta)], & \text{for } T_{min} < T_B < T_{max} \\ T_{avg} - T_B, & \text{for } T_B < T_{min} \end{cases} \quad (1)$$

where temperature is assumed to vary sinusoidally and T_{max}, T_{min}, and T_{avg} are the maximum, minimum, and average daily temperatures (°C), respectively; $R = [(T_{max} - T_{min})/2]$, $\theta = \arcsin[(T_B - T_{avg})/R]$, and T_B is a base (or lower threshold) temperature selected for each species/location (Snyder, 1985). Start-dates for heat accumulation are either fixed, or, if a given species requires chilling (i.e. vernalization, when exposure to cold temperatures is required to release buds from dormancy), begin on the date that the required number of "chilling" units have accumulated (Sect. 2.1.2). Table 1 contains T_B and GDD thresholds applied to each species selected for simulation.

Species-specific GDD thresholds for non-oak species were chosen based on published values when available (e.g. De Melo-Abreu et al., 2004), as well as using pollen count data for Pasadena, CA for the years 2003–2009 (excluding 2007, when extended late-season rains likely reduced airborne pollen concentrations). GDD thresholds were determined by analysis of the pollen counts along with meteorological data for Pasadena for 2003–2009 obtained from two California Irrigation Management Information System automated weather stations located near Pasadena, CA (wwwcimis.water.ca.gov/cimis/data.jsp, downloaded online through the University of California Statewide Integrated Pest Management Program's California Weather Data and Products website www.ipm.ucdavis.edu/WEATHER/wxretrieve.html). Using genus-specific base temperatures and start-dates for heat accumulation (Table 1), daily cumulative GDD values were calculated using the Pasadena meteorological data for the years 2003–2006 and 2008–2009. The average GDD thresholds reached on

GMDD
6, 2325–2368, 2013

the day of peak pollen concentration (according to the pollen count data) for each genus across all years were computed and assigned as the GDD threshold values for each genus. When available, published species- or genus-specific GDD thresholds were compared with the values calculated empirically using the Pasadena data, and in cases where the two values differed, the empirically calculated values were used (since often published values were for similar, but not identical species to those included in STaMPS or were based on observations made in different climatic zones than the simulation area). For olives, excellent agreement (within 2 %) was observed between the GDD threshold values suggested by De Melo-Abreu et al. (2004) and the value calculated based on pollen count data for Pasadena. For two of the genera (i.e. *Morus* and *Platanus*), published heat threshold values for flowering were not available, so the approach outlined above using the Pasadena data was used instead.

García-Mozo et al. (2002) observed that GDD flowering thresholds in Mediterranean oak species vary as a function of T_B, and that, in oaks and some other tree species, T_B itself is also elastic and varies (mainly) according to average annual temperature. The T_B–GDD threshold relationship described in García-Mozo et al. (2002) was used to determine GDD threshold for oaks, although it was calibrated to the oak species present in the S. CA model domain since the García-Mozo et al. (2002) study focused on Mediterranean oak species found in Spain. Appendix A describes how oak phenological observations from several important oak species in the domain (provided courtesy of Walt Koenig, Cornell University, Ithaca NY) were combined with meteorological and pollen count data to calibrate the García-Mozo et al. (2002) T_B–GDD threshold relationship to California oak species. In addition to informing the relationship between GDD threshold and T_B for oaks, the oak phenological data provided by Koenig were also used to develop a parameterization to simulate variation in flowering among populations. This "variation-mimicking" parameterization is applied to all simulated species, including grasses, and normally-distributes the pollen available for release on the calculated flowering peak date over a two-week period (which was typical of the oak phenological observations and which collaborators in the present study have corroborated in their

GMDD
6, 2325–2368, 2013

observations of temporal trends in pollen count intensities for a number of species, not shown).

As noted in García-Mozo et al. (2002), base temperatures are fixed in some species and variable in others. A 1 km resolution gridded base temperature map of North America was developed using relationships between annual average air temperature, altitude, and base temperature derived from García-Mozo et al. (2002) for oak trees. These base temperatures were assigned to all tree species that have been observed to exhibit local phenological adaptations (i.e. *Quercus*, *Platanus*; Chuine and Cour, 1999), while inelastic species (e.g. *Olea*, De Melo-Abreu et al., 2004) are assigned constant base temperatures (Table 1). When T_B data were not available for a given tree species, T_B values were assigned based on whether or not the species has chilling requirements for flowering (Sect. 2.1.2), which resulted in mulberry (*Morus*) being assigned a variable base temperature while walnut (*Juglans*) was assigned a constant T_B since, like birch and olive trees, walnut trees require chilling in order to flower (e.g. Warmund et al., 2009).

2.1.2 Simulating the chilling requirement

In addition to heat requirements for flowering, many tree (and grass) species also have vernalization requirements in which exposure to cold temperatures releases buds from dormancy and accelerates the onset of flowering. Of the tree genera selected for simulation with chilling requirements for flowering (*Betula*, *Juglans*, and *Olea*), olives (*Olea europaea*) have been best studied since they are important not only economically but are also highly allergenic (Rodríguez et al., 2001). Simulations performed for the selected tree species that have chilling requirements (olive, walnut, and birch) follow the chill-heating model developed for olives from De Melo-Abreu et al. (2004). In this method, accumulation of chilling units is determined via a piecewise approximation using the ratio of actual hourly temperature data for a location to an optimal chilling temperature for a given species. Hourly temperatures can be supplied to STaMPS directly from the meteorological input data, or if hourly meteorological data are not available,

GMDD
6, 2325–2368, 2013

can be approximated from daily minimum and maximum temperatures and sunrise time using the method proposed by De Wit et al. (1978, see Appendix B). The chilling units are then calculated as:

$$\mathrm{cum_c} = \begin{cases} 0 & \text{if } T_H \le 0\,^{\circ}\mathrm{C} \\ T_H / T_{opt} & \text{if } 0 < T_H \le T_{opt} \\ 1 - (T_H - T_{opt}) \cdot ((1 + 0.56)/(T_{BP} - T_{opt})) & \text{if } T_{opt} < T_H \le T_{BP} \\ -0.56 & \text{if } T_{BP} < T_H \end{cases} \quad (2)$$

where $\mathrm{cum_c}$ is the cumulative chilling value, T_H is the hourly air temperature (°C), T_{opt} is the optimal temperature at which chilling occurs, and T_{BP} is a breakpoint temperature above which −0.56 chilling units are lost (De Melo-Abreu et al., 2004).

If temperatures are within a prescribed range, the chilling value is equal to the ratio of hourly temperature to an optimal chilling temperature. If temperatures are below this range, no chilling units accumulate. If temperatures are above the optimum threshold value but do not exceed a breakpoint temperature (defined as the temperature above which a constant number of chilling units are negated), the chilling value decreases and eventually becomes negative as temperatures approach the breakpoint temperature; and if the hourly temperature is above the breakpoint temperature, then chilling units are decreased by a constant value. Once the specified cumulative chilling threshold has been reached for a given species and location, GDD accumulation begins, using the GDD approach described in Sect. 2.1.1 (above).

For olive, walnut and birch species, we use the same optimum and breakpoint chilling temperature values as those selected for olives in De Melo-Abreu et al. (2004), since these values were calculated for a Mediterranean climatic region, and observations (e.g. Jato et al., 2007; Warmund et al., 2009) suggest that birch and walnut trees have similar optimal chilling temperatures as olives. A threshold chilling quantity of 58 chilling units was selected for walnuts (Warmund et al., 2009); 432 chilling units was assigned to olives (De Melo-Abreu et al., 2004) and was also assigned to birch (for which published values were not available). Data regarding optimal T_B values for

GMDD
6, 2325–2368, 2013

birch and walnuts from which GDD calculations can be made are sparse; therefore, the same base thermal temperature that was developed for olives (9.1 °C, De Melo-Abreu et al., 2004) was applied to birch and walnut species. The Pasadena pollen count data suggest the presence of several olive varieties with different thermal requirements for flowering: there are generally several maxima in a given season that do not appear to be correlated to precipitation events (Fig. 2). De Melo-Abreu et al. (2004) found that different olive cultivars have unique chilling and heating requirements, but since the datasets used to determine tree species composition for this study (described in Sect. 2.4) identified all olives present within the domain as simply "*Olea europaea*", we applied the average heating and cooling threshold values across all of the cultivars studied by De Melo-Abreu et al. (2004), which yielded the same threshold value that was calculated for olives using the Pasadena data (Table 1).

2.2 Predicting the timing of pollen season for grasses

Many temperate grasses have a vernalization or "primary induction" requirement for flowering, in which the shortened days and reduced temperatures observed in autumn/winter trigger the beginning of the reproductive cycle. Aamlid et al. (2000) demonstrated that the length of primary induction in different cultivars of perennial ryegrass (*Lolium perenne*) was directly proportional to the latitude of origin of the cultivar/ecotype, with more northerly ecotypes requiring shorter photoperiods to satisfy their primary induction requirements. Ryegrass and most other grasses also have a "long day requirement", which is met when longer photoperiods during the summer months combine with increased summertime temperatures. This is also known as the secondary induction period, and is when flowering occurs in most grass species.

In grasses, vernalization may be *quantitative*, where cold temperatures occurring prior to the flowering season affect the timing of flowering but not the fraction of plants that head, or *qualitative*, in which adequate chilling is required for flowering and suboptimal chilling can reduce the fraction of heads flowering (Gleichsner and Appleby, 1996). Some grass species, such as annual ryegrass, have no primary induction

GMDD
6, 2325–2368, 2013

requirement. For these species, only sufficiently warm temperatures are required for floral initiation. In STaMPS, the beginning of grass pollen season and factors affecting the timing and magnitude of pollen released from grasses is determined based on species, meteorological/climatic factors and, for some species, latitude.

About three fourths of the initial S. CA study domain (Fig. 1, lower right) is characterized by warm Mediterranean climate zones and warm desert regions. In these climate zones, grass vernalization is expected to be weak or entirely absent (Aamlid et al., 2000; Heide, 1994; Meyer et al., 2004), while much of the rest of the domain consists of cold, arid regions with little vegetation cover. The two grass species selected for initial simulation were *Bromus mollis* and *B. diandrus* as these are the most abundant grass species within the domain according to the available species composition datasets (Sect. 2.4). As vernalization in *B. diandrus* is quantitative and no data on vernalization were available for *B. mollis*, a quantitative vernalization response based on *B. diandrus* (Gleichsner and Appleby, 1996) is applied to both species (Table 2). The relationship between length of exposure to cold temperatures and days to flowering as modeled for *B. diandrus* is depicted in Fig. 3.

As for tree species with chilling requirements, STaMPS simulates de-vernalization in grasses, when exposure to higher-than-optimal temperatures during the normal chilling period (normally November–March) causes a reduction in accumulated chilling units. The threshold temperature above which grasses become de-vernalized (15 °C) is based on Gleichsner and Appleby (1996). A GDD threshold of 185 applied to *Bromus* grasses that experience no chilling is also based on Gleichsner and Appleby (1996), who found that plants that were not vernalized flowered ~ 53 days after germination when kept in a greenhouse environment with day and night temperatures of 21 °C and 16 °C, respectively. Assuming a threshold value of 15 °C, and using Snyder's (1985) formula for calculating degree days when the minimum temperature is above the selected threshold value, 53 days of minimum and maximum temperatures of 21 °C and 16 °C, respectively, yields a GDD value of 185.5. Since the life-strategy of grasses differs from that of trees, the simulation of the start of grass-pollen season is based on

GMDD
6, 2325–2368, 2013

the assumption that GDD accumulation begins on 1 March (at the end of the vernalization period) or the day when maximum chilling (up to 42 days) is reached. Future simulations performed for domains that contain allergenic grasses with qualitative vernalization requirements (e.g. *Lolium perenne*) will initially be based on observations of *Lolium perenne* (Aamlid et al., 2000), *Bromus tectorum* (Meyer et al., 2004), and *Poa* species (Heide, 1994).

2.3 Effect of precipitation on pollen production potential

The amount of pollen emitted to the atmosphere is a function of the pollen available for release. Regardless of the PFT, the magnitude of pollen available for release (P_a; production potential) in each gridded domain cell for a given species is determined as:

$$P_a = \varepsilon_{sp} \cdot \alpha_{P,TP} \cdot \gamma \quad (3)$$

where ε_{sp} is the species- or genus-specific pollen production capacity, or pool size (expressed as grains/unit area), or the associated average pollen production capacity for the PFT of a species (if no species- or genus-level data are available); $\alpha_{P,TP}$ is a coefficient with values between 0 and 1 that modifies the pool size according to either precipitation (α_P) or both temperature and precipitation (α_{TP}), and γ is the total area occupied by the species (Sect. 2.4). Species-specific pollen production capacities (ε_{sp}) derived from literature values (e.g. Hidalgo et al., 1999; Molina et al., 1996; Prieto-Baena et al., 2003; Sütyemez, 2007) were compiled into a database of allergenic vegetation species. This database also includes relative allergenicities (expressed as severe, moderate, mild, or unknown) for each species.

The amount of pollen produced by Mediterranean tree species is affected by precipitation a full year or more prior to pollen release (Fairley and Batchelder, 1986) and, in non-Mediterranean temperate climatic zones, both precipitation and temperature up to a year prior to blooming can impact the magnitude of tree pollen produced depending on the species (Kozlowski, 1971; Miyazaki et al., 2009). For grasses, precipitation within a given growing season appears to be the most important determinant for pollen

GMDD
6, 2325–2368, 2013

production within that season (Craine et al., 2010). For this study, monthly average precipitation within the domain was determined using 30 arc second resolution monthly average precipitation data for the 1971–2000 period (PRISM Climate Group, Oregon State University, http://prism.oregonstate.edu, created 4 February 2004).

For trees, observed (or simulated) precipitation data a full year prior to the start of the simulation period are compared with average precipitation (and early-season chilling, for tree species with quantitative chilling requirements including *Betula* and *Olea* species) values for the wet season (defined as 1 October to 30 April for the study domain) to estimate the total amount of pollen available for release by a given tree species. This ratio is used to compute a coefficient which modifies the pool of pollen available for release, and is based on the work of Fairley and Batchelder (1986), who studied the relationship between rainfall and observed pollen counts in San Francisco and San Jose, CA between 1973 and 1981. In particular, Fairley and Batchelder's San Jose rainfall and pollen count data (Fig. 4) were applied since the San Jose pollen counting station used in that study was closer to the actual source trees than the San Francisco station (Fairley and Batchelder, 1986). Data for average wet season precipitation over the San Jose area were obtained by summing the PRISM model average monthly precipitation (1971–2000) for the months of October–April and then taking the average of all PRISM pixels located within the San Jose census tract zone (geospatial census tract data for the city of San Jose were obtained from http://www.sanjoseca.gov). The relationship between precipitation and pollen potential for oak and other trees without quantitative vernalization requirements is expressed as:

$$\alpha_P = 0.06e^{3.53(x_t)} \quad (4)$$

where α_P is a dimensionless coefficient modifying pollen potential and x_t is the ratio between total wet season precipitation and average total wet season precipitation.

This general approach is also used for grasses, but the window of time for which precipitation is summed is the 80-day period prior to onset of flowering (rather than

GMDD
6, 2325–2368, 2013

wet-season precipitation a year prior to the simulation period), based on the work of Craine et al. (2010). The precipitation-driven pollen production coefficient (γ_p) for grasses is:

$$\begin{aligned} &\text{For } x_g \le 0, && \gamma_p = 0 \\ &\text{For } 0 < x_g < 0.51, && \gamma_p = 0.0141 x_g \\ &\text{For } 0.51 \le x_g, && \gamma_p = 2.0262 x_g - 1.0262 \end{aligned} \quad (5)$$

where x_g is the fraction of average precipitation experienced over the 80 day period prior to the start date of flowering.

It should be noted that the information used to derive the grass precipitation coefficient is based on 25 yr of observations at a prairie grassland in Kansas (in Midwestern US), and the intercept of the equation (i.e. the threshold where flowering is zero) is ~ 0.51, so that, in years with 51 % or less of the average precipitation, there would theoretically be no grass pollen produced. It would be expected that the precipitation threshold below which grass species cannot flower is a function of species-specific minimum precipitation requirements as well as the amount of elasticity a species is capable of exhibiting in terms of local adaptations to climate. Since there is little information regarding these considerations for grasses, the STaMPS model assumes that in years with low precipitation, grass pollen production approaches zero only as the accumulated precipitation also approaches zero. This assumption allows some grass pollen to be produced during low-precipitation years, since even in arid regions, some locations can still receive sufficient rainfall, and as a result, grass pollen is frequently still observed in arid regions during dry years (Cariñanos et al., 2004).

The occurrence of rain events close to and during grass pollen season is also known to prolong the flowering season (Cariñanos et al., 2004). Neither of the grass species selected for simulation were included in the Cariñanos study, therefore precipitation effects on the length of the grass pollen season were excluded.

For olives and other tree species with qualitative vernalization requirements, an algorithm was developed to describe the dual effects of late-autumn chilling and

GMDD
6, 2325–2368, 2013

precipitation on pollen production. This algorithm calculates a dimensionless coefficient that modulates pollen-production potential, and uses daily temperature data for the month of November (in the autumn prior to pollen season) as well as precipitation data for the wet season in the year prior to the current flowering period (as described above).

The dual vernalization/precipitation coefficient (α_{TP}) was developed using meteorological data and olive pollen counts for Pasadena, CA, for the years 2003–2006 and 2008–2009, (but excluding 2007 since extended rains between March–May likely reduced airborne pollen concentrations for a number of species), which indicated a strong relationship ($R^2 \sim 0.99$) between early season chilling and observed peak olive pollen counts, with additional influence from prior-year wet season precipitation (Fig. 5). The effect of early-season vernalization alone explained ~ 75 % of the observed variability in peak pollen counts, while prior-year wet season precipitation alone explained very little (~ 7 %) of the variability.

The vernalization/precipitation coefficient for trees with quantitative chilling requirements is expressed as:

$$\alpha_{TP} = \left(6.777 \cdot \left(x_t^{1.575}\right) \cdot C_f\right) + 0.715 \quad (6)$$

where x_t is the ratio between total wet season precipitation and average total wet season precipitation (as in Eq. 5), C_f is accumulated chilling units for the period 1 November to 30 November divided by the total expected chilling needed for the species to satisfy its chilling requirements. As there is insufficient data with which to extrapolate an upper-limit on pollen production potentials in tree species, α_{TP} is capped at 2.5, based on the largest increase in tree pollen observed in response to precipitation (Fairley and Batchelder, 1986), as well as observations of birch trees made by Jato et al. (2007), where the largest observed change in pollen production was a factor of ~ 2. The vernalization/precipitation coefficient was used for birch and olive species; pollen production potential for walnut species is calculated on wet season precipitation alone as these species have relatively low chilling requirements (Warmund et al., 2009).

GMDD
6, 2325–2368, 2013

2.4 Determination of species composition and fractional vegetation cover

To create pollen potential emission estimates for use in 3-dimensional models, spatially-explicit maps of the pollen-producing species are needed. The data sources used to determine species composition and fractional PFT cover for each STaMPS PFT vary according to the land cover classes present in each domain cell (Table 3). Fractional land cover class membership within each cell was determined using the USDA National Agriculture Statistics Service Cropland Data Layer (NASS CDL; http://www.nass.usda.gov/research/Cropland/SARS1a.htm; Johnson and Mueller, 2010) product, which was also used to assign species composition for fractions of cells containing agricultural allergenic classes including walnut orchards.

Urban tree inventories were used to assign species compositions to urban cell fractions. Tree inventory data were obtained for Long Beach, CA, Riverside, CA, Los Angeles, CA, Berkeley, CA, San Francisco, CA, Modesto, CA and Reno, NV. Cells containing urban tree cover located in the southern half of CA were assigned the average weighted species compositions based on the Long Beach, Riverside and Los Angeles inventories, while those located in the northern half of the state and extreme southern Oregon were assigned weighted averages from the Berkeley, San Francisco, and Modesto inventories. All urban cells located in Nevada and surrounding states to the north and west were assigned the weighted average species composition computed using the Reno inventory. Section 4.1 discusses the uncertainties and limitations associated with deriving urban tree species compositions from urban tree inventories.

For forested land cover classes, species composition is assigned using Forest Inventory and Analysis (FIA, http://www.fia.fs.fed.us/) data and (for areas characterized by significant shrubby tree cover such as the scrub oak woodlands of S. CA) Natural Resource Conservation Service (NRCS, http://soildatamart.nrcs.usda.gov/) data. NRCS data were also used to assign species compositions in open space and shrubland zones and open space/grassland areas, while the CDL NASS data was used for agricultural locations. FIA and NRCS species composition datasets were averaged

GMDD
6, 2325–2368, 2013

across US EPA level III or IV ecoregions (http://www.epa.gov/wed/pages/ecoregions/level_iii_iv.htm) to provide continuous species distribution maps, as the FIA data are plot-level inventories and not all of the NRCS polygons contained species composition information.

Vegetation and land cover products derived from the NLCD tree canopy and impervious ground cover datasets (http://www.epa.gov/mrlc/nlcd-2001.html) and land use by class (based on the CDL dataset) were used to determine fractional tree and non-tree vegetation cover. In some cases, these datasets are unreliable, especially in highly-heterogeneous areas including most urban locations. For example, the NLCD canopy cover dataset suggests virtually zero tree cover over much of the city of Long Beach, CA. However, estimates of fractional tree and non-tree cover for urban locations in this area made using aerial imagery and a visually-supervised digital method as described in Duhl et al. (2012; Table 4) are non-negligible. These urban vegetation cover estimates for STaMPS were assigned to all urban CDL land cover classes within the study domain.

Fractional cover by allergenic species (γ) is determined within each grid cell using the fractional vegetation cover estimates combined with species composition data derived from the sources described above. Species-specific vegetation cover estimates (in m^2) for the selected species are then multiplied by species-specific pollen production capacity (ε_{sp}) and modified by either the precipitation-driven pollen production coefficient (α_P) or the combined temperature/precipitation pollen production coefficient (α_{TP}) to determine the amount of pollen produced by each species within each grid cell (as described in Sect. 2.3).

2.5 Model domains and meteorological data used for current and future simulations

Initial STaMPS and pollen transport simulations were performed for a 4 km resolution model domain centered over southern California (Fig. 1, lower right corner) for 1 March through 30 June 2010. This domain and time period coincided with an extensive set

GMDD
6, 2325–2368, 2013

of pollen observations collected as part of the University of Southern California's Children's Health Study from which ambient pollen count data were collected and were used to evaluate and optimize STaMPS. The reader is referred to Zhang et al. (2013a) for a detailed description of how STaMPS output is incorporated into a regional pollen transport model and for model evaluation results. A larger 12 km outer domain (Fig. 1), which was used to provide boundary conditions for the 4 km simulations in Zhang et al. (2013a), was used to investigate the impact of climate change on pollen emission potential.

To simulate the climate change impact, meteorological fields used as input to STaMPS were downscaled from the results of the ECHAM5 global climate model (Roeckner et al., 1999, 2003) using the WRF model (Skamarock et al., 2008; http://www.wrf-model.org). The WRF model is a state-of-the-science mesoscale weather prediction system suitable for a broad spectrum of applications ranging from meters to thousands of kilometers, and has been developed and used extensively for regional climate modeling (e.g. Leung et al., 2006).

In this study, WRF was applied with nested 108 km and 36 km horizontal resolution domains, centered over the continental United States, with 31 vertical layers. The 12 km domain was constructed so that its cell boundaries were aligned with the 36 km domain (i.e., each 36 km cell within the domain contained a 3×3 array of 12 km cells, and each of these were forced with the meteorological data for the 36 km cell containing them). The ECHAM5-driven WRF simulations for the historical period have been shown to represent the ENSO (El Nino–Southern Oscillation) patterns and extreme temperature and precipitation over the western US reasonably well (Zhang et al., 2012; Dulière et al., 2011). The 36 km WRF simulation results used here have been applied to study the impact of global change on regional air quality in the US (Avise et al., 2012). Two 10-yr monthly mean 36 km WRF temperature and precipitation results were used to drive STaMPS to evaluate the projected change in pollen emission potentials in the outer domain shown in Fig. 1 from 1995–2004 to 2045–2054 under the Intergovernmental Panel on Climate Change (IPCC) Special Report on Emissions Scenarios (SRES) A1B

GMDD
6, 2325–2368, 2013

scenario, which assumes balanced progress along all resource and technological sectors, resulting in a balanced increase in greenhouse gas concentrations from 2000 to the 2050s (Nakicenovic et al., 2000). Two-sample t tests were used to verify whether observed differences in current vs. future simulations were significant for both pollen production and start date of flowering. Prior to running the t tests, F tests were performed on each variable tested. When the results of the F tests indicated that variance was not significantly different (for $\alpha = 0.01$), variances were pooled for the t test calculations.

3 Results of current and future simulations

Table 5 presents the differences in the simulated magnitude and timing of pollen season for the selected species between the current and future scenarios. Across all modeled species, pollen season starts 5–6 days earlier, on average, in the future simulations, with the future simulations showing a domain-wide average annual temperature increase of $\sim 1\,^{\circ}\mathrm{C}$ (Fig. 6). The advance in flowering time simulated by STaMPS in response to temperature increase is in the observationally-derived range reported for early-spring blooming tree species (Črepinšek et al., 2012; Frei, 1998; Fitter and Fitter, 2002) as well as from other simulations (e.g. De Melo-Abreu et al., 2004).

The effects on pollen production potential (P_a) in species with chilling requirements between the current vs. future scenarios were much more variable depending on the species/genera considered. For birch and olive (*Betula* and *Olea*), which have the highest chilling requirements, P_a exhibits a 3–4 % decrease in the future simulations. For walnuts (*Juglans*) there is essentially no change in pollen production. Much of the change in pollen production predicted for birch and olive species can be attributed to the chilling-precipitation coefficient applied to chilling species, since a comparable or even higher proportion of cells containing these trees met thermal requirements (and therefore began flowering) before the end of the simulation period (30 June) in the future compared to current scenarios (Table 6). The chilling-precipitation coefficients

GMDD
6, 2325–2368, 2013

applied to the chilling species as calculated across the domain for the two climate scenarios indicate that, for the future simulation, less precipitation combined with less early season chilling (occurring in November, the period that was found to be critical for pollen production) compared to the current scenario also led to smaller pools for *Betula* and *Olea*. This result contrasts with the predictions of Zhang et al. (2013b) that peak birch pollen concentrations could increase by a factor of up to 7–8 by 2100 in northeastern US. *Juglans*, which has extremely low chilling requirements as compared to birch and olive species, was treated as a non-chilling species for the purposes of simulating P_a (since the entirety of this species' chilling requirements are almost always met by the end of November), though the timing of pollen season for *Juglans* was calculated as described for other chilling species.

Across most of the non-chilling tree species, P_a either decreased or did not change a lot, although the observed differences were statistically significant (Table 5). We attribute most of the reduction in P_a simulated for the future scenario to the lower precipitation values projected during the October–April wet season in the future scenario, since (as was the case for the chilling species) higher proportions of cells reached species-specific thermal thresholds for flowering before the end of simulation period (30 June) in the future compared to current simulation (Table 6). Among the simulated species, late-blooming oaks were singular in that a substantial increase (9 %) in simulated pollen production was forecast for this group. Since these species experienced the same precipitation as other species (and therefore effects from the precipitation coefficient are not expected to influence the simulated differences), we attribute this increase to a temporal shift in flowering time for the late-blooming species, which would cause a higher percentage of these late-blooming species to flower before the end of the simulation period in the future versus current simulations, and which is reflected in the proportion of cells flowering between March–June in the two scenarios in Table 6. It should be emphasized that the simulated differences in P_a between future and current scenarios should not be interpreted as absolute differences in production since (as noted above) these simulations are for a limited time period and therefore some of

GMDD
6, 2325–2368, 2013

the observed differences for some cells/species can be attributed to shifts in flowering time into or outside of the simulation period.

4 Discussion and conclusions

4.1 STaMPS model evaluation, uncertainties and limitations

To evaluate STaMPS, output for a validation period (1 March–30 June 2010) was used as input for a pollen dispersal model to generate pollen concentrations for the 4 km (S. CA) domain as described in a companion paper (Zhang et al., 2013a). The simulated concentrations were compared with observed pollen count data for that time period from nine sites. For most of the species/locations within the domain where comparisons were made, the temporal trend of the pollen potential was reasonably good and resultant simulated concentrations agreed moderately well with observations, although most notably there are underestimates in simulated walnut pollen concentrations, overestimates in grass pollen concentrations, and either over- or underestimates in oak pollen concentrations depending on location (Zhang et al., 2013a).

The accuracy of the various datasets used to assign species composition within the domain is a large source of uncertainty in the simulated magnitudes of pollen produced by each species. The STaMPS model evaluation efforts described in Zhang et al. (2013a), for example, suggest that either the pollen production capacity (ε_{sp}) assigned to walnuts was too low or that walnut trees may be more prevalent within the domain than indicated from the land cover data available for the domain (or both). Other than the agricultural walnut orchards indicated to be present within the study region (mostly within California's Central Valley), urban tree inventories suggest that walnuts are present but comprise < 0.1 % of urban trees. Urban tree inventories generally only include trees maintained by municipalities (such as trees growing along city streets). If private property owners favored walnut trees on their properties more than municipalities, the actual fraction contributed to the total urban canopy by walnuts

GMDD
6, 2325–2368, 2013

would be higher than indicated by the inventories. Uncertainties associated with the other datasets used to assign species composition to the domain cells (FIA, NRCS, etc.) may be significant but have not been quantified. The satellite-derived fractional vegetation cover estimates used to determine vegetation cover within the domain have much lower uncertainties (most likely these are within 15 %; Duhl et al., 2012).

The pollen production potential coefficients assigned to each species (Sect. 2.3) were derived from the literature, and there are large ranges in observed pollen production for some genera, e.g. three orders of magnitude for different walnut cultivars (Sütyemez, 2007). It is difficult to determine whether differences between simulated and observed pollen concentrations arise from uncertainties in species distribution data, incorrect pollen production coefficients, or from observationally-derived errors (e.g. a pollen counting station may not receive prevailing winds from the direction of tree populations flowering in an area, precipitation events may cause pollen washout, etc.). Despite these limitations, our study is the first to predict pollen production for multiple species in the western half of the US, and therefore STaMPS improves capabilities for predicting pollen season in the long term. Nonetheless, these limitations should be kept in mind when interpreting the pollen dispersal results.

As mentioned in Sect. 3, simulated differences in pollen production between future and current scenarios should not be interpreted as absolute differences in production since these simulations have been run for a limited flowering period and therefore some of the observed differences in production can be attributed to shifts in flowering time into or outside of the simulation period for some cells/species. To get a more comprehensive picture of total predicted pollen production under current versus future simulations, a longer simulation period is suggested.

Due to the scarcity of species-specific data in the literature, all species within each genus simulated by STaMPS are currently assigned the same pollen production capacity coefficients and GDD threshold values for flowering. Therefore, there will be some loss of resolution in the simulated temporal pattern of pollen production if some species have unique thermal requirements for flowering (which is widely reported in the

GMDD
6, 2325–2368, 2013

literature but difficult to determine in practice since for many species pollen is stenopalinous, i.e. cannot be differentiated at a given taxonomic level). This can be improved by characterizing GDD thresholds using phenological observations as well as developing improved species distribution datasets (e.g. making identifications at the variety/cultivar level when appropriate, etc.).

In regions of significant topographical variability, like S. CA in this study, domain cell size should be selected with a consideration of the potential effect on the predicted timing and magnitude of pollen season arising from averaging temperature and precipitation gradients within domain cells which may be heterogeneous due to topography. These considerations should take into account (1) the relative sensitivity of this model (i.e. average flowering date among early spring to summer-blooming species advances 5–6 days with a corresponding average domain-wide annual temperature increase of 1 °C), (2) the range of elevations that are present within domain cells at various cell sizes, (3) the response of temperature and precipitation to changes in elevation (such as the lapse rate of temperature with respect to altitude, etc.), and (4) the required accuracy needed for the simulations in question.

Across the 12 km domain, the average (standard deviation) range of elevations (using a 1 km-resolution elevation dataset) was 566 (396) m. Applying the dry adiabatic lapse rate of 9.8 °C km^{-1} and assuming a linear relationship between temperature and flowering time sensitivity among the modeled species, we estimate that actual pollen season start dates for the spring and early summer-blooming species within a topographically-diverse grid cell may occur over a period of 31 ± 27 days. These rather broad ranges would likely not be useful for applications requiring precise temporal predictions but for the present study (a comparison between simulated future vs. current pollen seasons), the focus was on the differences between two scenarios, so this cell size was acceptable. For the evaluation of the STaMPS model as described in Zhang et al. (2013a), as well as for the purposes of the broader study assessing human health impacts from pollen and adjuvant air pollutants (to be presented in future publications), a smaller 4 km domain (Sect. 2.5) was used, and should provide more

GMDD
6, 2325–2368, 2013

accurate predictions of flowering time due to a smaller range of elevations within these cells as compared to the 12 km cells.

4.2 Conclusion and plans for future model development

The Simulator of the Timing and Magnitude of Pollen Season (STaMPS) model simulates the timing and production of wind-dispersed allergenic pollen by terrestrial, temperate vegetation as part of a broader study of how pollen occurrence may be affected by climate change and interact with anthropogenic pollutants to affect human health. The STaMPS model has been initially designed to simulate the release of pollen in a domain centered over Southern California, characterized by moderate Mediterranean and oceanic climate zones as well as regions of arid desert and arid steppe.

Simulations performed using ECHAM5-WRF meteorological model output for current (1995–2004) and future (2045–2054) climate scenarios indicate that all of the spring to early summer-blooming tree and grass species selected for initial simulations flower 5–6 days earlier under an average annual domain-wide temperature increase of $\sim 1\,^{\circ}C$, while effects on pollen production in these scenarios varied by species and were affected by the selected simulation time period. It should be kept in mind that the WRF-ECHAM5 meteorological fields used to drive the future simulations assume a balanced increase in greenhouse gas concentrations from 2000 to the 2050's, so when comparing these results to other simulations of future pollen production, the future climate scenarios used in the simulations must be considered.

Planned future simulations include allergenic shrub species and additional climatic zones. This will include *Artemesia* (sagebrush) species, as sagebrush pollen is frequently observed at some of the pollen counting stations participating in the Children's Health Study. For the initial model simulation period (March–June 2010), no pollen emissions from shrubs were included, as both ragweed and sagebrush pollen seasons generally start in late summer or early fall (Laursen et al., 2007; Peternel et al., 2006). Module development is also planned for additional grass species including Bermuda

GMDD
6, 2325–2368, 2013

grass (*Cynodon dactylon*), perennial ryegrass (*Lolium perenne*) and/or Timothy grass (*Phleum pratense*).

Efforts to predict the timing and magnitude of pollen season would be bolstered by increasing the number of pollen counting stations and making these data publicly available. Although there is a large amount of pollen data collected, it is not available at an affordable cost. The paucity of freely-available observational data for the study domain has stymied efforts to validate simulations for many locations. This lack of observational data is compounded by the stenopalinous nature of pollen for many species, which reduces the species-resolution of pollen counts obtained via traditional counting methods. The development of new techniques for identifying pollen at the species level or increasing phenological observations for important species would also provide much-needed data that could be used both to develop species-specific model parameterizations as well as in model validation efforts and would serve to increase confidence in the predictive ability of the STaMPS model, although this is the first effort to simulate pollen season for a large number of species in the western US and therefore is a step forward in simulating the reproductive response of vegetation to climate change.

Appendix A

Calculation of GDD threshold values for oak trees

The T_B–GDD threshold relationship described in García-Mozo et al. (2002) was used to determine GDD threshold for oaks, although it was calibrated to the oak species present in the S. CA model domain since the García-Mozo et al. (2002) study focused on Mediterranean oak species found in Spain. Phenological observations of oak flowering dates for three important California oak species (*Q. agrifolia*, *Q. lobata*, *Q. douglasii*) known to be present in the model domain were collected from 1991–1996 and 2009–2011 at the Hastings Biological Field Station (in Monterrey County, CA) and the Sedgwick Reserve (in Santa Barbara County, CA) and were provided

GMDD
6, 2325–2368, 2013

courtesy of Walt Koenig (Cornell University, Ithaca NY). Meteorological data for Hastings Biological Field Station (http://www.hastingsreserve.org) and Sedgwick Reserve (http://sedgwick.ucnrs.org) were obtained and combined with the phenological observations to determine the relationship between GDD and base temperature for oaks within the domain (Table 1). The Pasadena, CA pollen count data indicated that oak pollen season frequently has a bi-modal distribution with peaks observed in March–early April and again in May. The oak species present within the domain were therefore lumped into two groups (early-blooming and late-blooming, Table 1) according to the phenological observations provided for *Q. agrifolia*, *Q. lobata* and *Q. douglasii*, and qualitative time-of-flowering data obtained for all other species from the NRCS USDA Plants Database (http://plants.usda.gov/java/).

For domain cells with T_B values of 7.3 °C or higher, the slope of the García-Mozo et al. (2002) GDD–T_B algorithm was used to predict the flowering GDD threshold for early blooming oaks, although a different intercept was selected to calibrate the simulated flowering predictions within the study domain. The intercept was determined by plotting the observed pollen count and phenological data against observed cumulative GDD for the available locations with oak data (i.e. Pasadena, CA and the study sites described above). For later-blooming oaks, the algorithm used to determine the threshold GDD value upon which flowering occurs was developed using pollen count data for Pasadena, CA, for the years 2003–2006 and 2008–2009 and an accumulation period beginning on 1 February each year.

For non-oak species in STaMPS, GDD flowering thresholds do not vary according to T_B, but are assumed as constant values since insufficient data exist from which to determine whether accumulated GDD flowering threshold values are a function of base temperature.

GMDD
6, 2325–2368, 2013

Appendix B

Method used to estimate hourly temperatures (De Wit et al., 1978) using daily minimum and maximum temperatures and sunrise time

For $0 \le H < H_{rise}$ and $1400\,h < H \le 2400\,h$, $T_H = T_{avg} + R \cdot (\cos(\pi H' / (10 + H_{rise})))$

For $H_{rise} \le H \le 1400\,h$, $T_H = T_{avg} - R \cdot (\cos(\pi (H - H_{rise}) / (14 - H_{rise})))$

where H is the local hour; T_H is the simulated hourly temperature (°C); $T_{avg} = (T_{min} + T_{max})/2$; T_{min} and T_{max} are the daily minimum and maximum temperatures, respectively; $R = (T_{max} - T_{min})/2$, H_{rise} is the sunrise time, and $H' = H + 10$ for $0 \le H < H_{rise}$ and $H - 14$ for $1400\,h < H \le 2400\,h$. This method was compared to several other techniques for approximating hourly temperature by Reicosky et al. (1989) and was selected because it was the best method in that study.

Acknowledgements. The National Center for Atmospheric Research is sponsored by the US National Science Foundation. The authors acknowledge support from US EPA STAR Grant R834358. The authors also thank urban planners and GIS offices within the communities of Long Beach, CA, Riverside, CA, and Reno, NV for providing tree inventory data and Walt Koenig at Cornell University for providing his phenological oak data.

References

Aamlid, T. S., Heide, O. M., and Boelt, B.: Primary and secondary induction requirements for flowering of contrasting European varieties of *Lolium perenne*, Ann. Bot.-London, 86, 1087–1095, doi:10.1006/anbo.2000.1275, 2000.

Akinbami, L. J., Moorman, J. E., and Liu, X.: Asthma prevalence, health care use, and mortality: United States, 2005–2009, National Health Statistics Reports, 32, National Center for Health Statistics, Hyattsville, MD, 15 pp., 2011.

Avise, J., Gonzalez-Abraham, R., Chung, S. H., Chen, J., Lamb, B., Salathé, E. P., Zhang, Y., Nolte, C. G., Loughlin, D. H., Guenther, A., Wiedinmyer, C., and Duhl, T.:

GMDD
6, 2325–2368, 2013

Evaluating the effects of climate change on summertime ozone using a relative response factor approach for policymakers, J. Air Waste Ma. Assoc., 62, 1061–1074, doi:10.1080/10962247.2012.696531, 2012.
Cariñanos, P., Galan, C., Alcázar, P., and Domínguez, E.: Airborne pollen records response to climatic conditions in arid areas of the Iberian peninsula, Environ. Exp. Bot., 52, 11–22, 2004.
Centers for Disease Control and Prevention (CDCP): Asthma in the US, Vital Signs, available at: http://www.cdc.gov/vitalsigns/Asthma/, last access: 24 May 2012, 2011.
Chuine, I. and Cour, P.: Climatic determinants of budburst seasonality in four temperate-zone tree species, New Phytol., 143, 339–349, doi:10.1046/j.1469-8137.1999.00445.x, 1999.
Craine, J. M., Towne, E. G., and Nippert, J. B.: Climate controls on grass culm production over a quarter century in a tallgrass prairie, Ecology, 91, 2132–2140, 2010.
Črepinšek, Z., Štampar, F., Kajfež-Bogataj, L., and Solar, A.: The response of *Corylus avellana* L. phenology to rising temperature in north-eastern Slovenia, Int. J. Biometeorol., 56, 681–694, doi:10.1007/s00484-011-0469-7, 2012.
De Melo-Abreu, J. P., Barranco, D., Cordeiro, A. M., Tous, J., Rogado, B. M., and Villalobos, F. J.: Modelling olive flowering date using chilling for dormancy release and thermal time, Agr. Forest Meteorol., 125, 117–127, 2004.
De Wit, C. T., Goudriaan, J., van Laar, H. H., Penning de Vries, F. W. T., Rabbinge, R., van Keulen, H., Sibma, L., and de Jonge, C.: Simulation of assimilation, respiration and transpiration of crops, Simulation Monographs, Pudoc, Wageningen, The Netherlands, 141 pp., 1978.
Duhl, T. R., Guenther, A., and Helmig, D.: Estimating urban vegetation cover fraction using Google Earth® images, J. Land Use Sci., 7, 311–329, doi:10.1080/1747423X.2011.587207, 2012.
Dulière, V., Zhang, Y., and Salathé, E. P.: Extreme precipitation and temperature over the US Pacific Northwest: a comparison between observations, reanalysis data, and regional models, J. Climate, 24, 1950–1964, doi:10.1175/2010JCLI3224.1, 2011.
Fairley, D. and Batchelder, G. L.: A study of oak-pollen production and phenology in northern California: prediction of annual variation in pollen counts based on geographic and meterologic factors, J. Allergy Clin. Immun., 78, 300–307, 1986.
Fitter, A. H. and Fitter, R. S. R.: Rapid changes in flowering time in British plants, Science, 296, 1689–1691, 2002.

GMDD
6, 2325–2368, 2013

Frei, T.: The effects of climate change in Switzerland 1969–1996 on airborne pollen quantities from hazel, birch, and grass, Grana, 37, 172–179, doi:10.1080/00173139809362662, 1998.
Frenguelli, G. and Bricchi, E.: The use of the pheno-climatic model for forecasting the pollination of some arboreal taxa, Aerobiologia, 14, 39–44, 1998.
Frenguelli, G., Tedeschini, E., Veronesi, F., and Bricchi, E.: Airborne pine (*Pinus* spp.) pollen in the atmosphere of Perugia (central Italy): behaviour of pollination in the two last decades, Aerobiologia, 18, 223–228, 2002.
García-Mozo, H., Galán, C., Aira, M. J., Belmonte, J., Diáz de la Guardia, C., Fernández, D., Gutierrez, A. M., Rodriguez, F. J., Trigo, M. M., and Dominguez-Vilches, E.: Modelling start of oak pollen season in different climatic zones in Spain, Agr. Forest Meteorol., 110, 247–257, 2002.
Gilmour, M. I., Jaakkola, M. S., London, S. J., Nel, A. E., and Rogers, C. A.: How exposure to environmental tobacco smoke, outdoor air pollutants, and increased pollen burdens influences the incidence of asthma, Environ. Health Persp., 114, 627–633, doi:10.1289/ehp.8380, 2006.
Gleichsner, J. A. and Appleby, A. P.: Effects of vernalization on flowering in ripgut brome (*Bromus diandrus*), Weed Sci., 44, 57–62, 1996.
Greenwood, V.: Why are asthma rates soaring?, Sci. Am., 304, 32–33, 2011.
Guenther, A., Karl, T., Harley, P., Wiedinmyer, C., Palmer, P. I., and Geron, C.: Estimates of global terrestrial isoprene emissions using MEGAN (Model of Emissions of Gases and Aerosols from Nature), Atmos. Chem. Phys., 6, 3181–3210, doi:10.5194/acp-6-3181-2006, 2006.
Guenther, A. B., Jiang, X., Heald, C. L., Sakulyanontvittaya, T., Duhl, T., Emmons, L. K., and Wang, X.: The Model of Emissions of Gases and Aerosols from Nature version 2.1 (MEGAN2.1): an extended and updated framework for modeling biogenic emissions, Geosci. Model Dev., 5, 1471–1492, doi:10.5194/gmd-5-1471-2012, 2012.
Heide, O. M.: Control of flowering and reproduction in temperate grasses, New Phytol., 128, 347–362, 1994.
Hidalgo, P. J., Galán, C., and Domínguez, E.: Pollen production of the genus *Cupressus*, Grana, 38, 296–300, 1999.
Jato, V., Rodríguez-Rajo, F. J., and Aira, M. J.: Use of phenological and pollen-production data for interpreting atmospheric birch pollen curves, Ann. Agr. Env. Med., 14, 271–280, 2007.

GMDD
6, 2325–2368, 2013

Johnson, D. M. and Mueller, R.: The 2009 cropland data layer, Photogramm. Eng. Rem. S., 76, 1201–1205, 2010.
Kozlowski, T. T.: Growth and Development of Trees, vol. 2: Cambial Growth, Root Growth, and Reproductive Growth, Academic Press, New York, 514 pp., 1971.
Laursen S. C., Reiners, W. A., Kelly, R. D., and Gerow, K. G.: Pollen dispersal by *Artemesia tridentata* (Asteraceae), Int. J. Biometeorol., 51, 465–481, 2007.
Leung, L. R., Kuo, Y.-H., and Tribbia, J.: Research needs and directions of regional climate modeling using WRF and CCSM, B. Am. Meteorol. Soc., 87, 1747–1751, 2006.
Meyer, S. E., Nelson, D. L., and Carlson, S. L.: Ecological genetics of vernalization response in *Bromus tectorum* L. (Poaceae), Ann. Bot.-London, 93, 653–663, 2004.
Miyazaki, Y., Osawa, T., and Waguchi, Y.: Resource level as a proximate factor influencing fluctuations in male flower production in *Cryptomeria japonica* D. Don., J. For. Res.-Japan, 14, 358–364, 2009.
Molina, R. T., Rodríguez, A. M., Palaciso, I. S., and López, F. G.: Pollen production in anemophilous trees, Grana, 35, 38–46, doi:10.1080/00173139609430499, 1996.
Nakicenovic, N., Alcamo, J., Davis, G., de Vries, B., Fenhann, J., Gaffin, S., Gregory, K., Grübler, A., Jung, T. Y., Kram, T., La Rovere, E. L., Michaelis, L., Mori, S., Morita, T., Pepper, W., Pitcher, H., Price, L., Riahi, K., Roehrl, A., Rogner, H.-H., Sankovski, A., Schlesinger, M., Shukla, P., Smith, S., Swart, R., van Rooijen, S., Victor, N., and Dadi, Z.: IPCC Special Report on Emissions Scenarios, Cambridge University Press, Cambridge, UK, 2000.
Nathan, R. A.: The burden of allergic rhinitis, Allergy Asthma Proc., 28, 3–9, 2007.
Peternel, R., Čulig, J., Hrga, I., and Hercog, P.: Airborne ragweed (*Ambrosia artemisiifolia* L.) pollen concentrations in Croatia, 2002–2004, Aerobiologia, 22, 161–168, 2006.
Prieto-Baena, J. C., Hidalgo, P. J., Domínguez, E., and Galán, C.: Pollen production in the Poaceae family, Grana, 42, 153–160, 2003.
PRISM Climate Group, Oregon State University: available at: http://prism.oregonstate.edu, last access: 15 August 2012 created 4 February 2004.
Reicosky, D. C., Winkelman, L. J., Baker, J. M., and Baker, D. G.: Accuracy of hourly air temperatures calculated from daily minima and maxima, Agr. Forest Meteorol., 46, 193–209, 1989.
Rodríguez, R., Villalba, M., Monsalve, R. I., and Batanero, E.: The spectrum of olive pollen allergens, Int. Arch. Allergy Imm., 125, 185–195, 2001.

GMDD
6, 2325–2368, 2013

Roeckner, E., Bengtsson, L., Feichter, J., Lelieveld, J., and Rodhe, H.: Transient climate change simulations with a coupled atmosphere-ocean GCM including the tropospheric sulfur cycle, J. Climate, 12, 3004–3032, doi:10.1175/1520-0442(1999)012<3004:TCCSWA>2.0.CO;2, 1999.

Roeckner, E., Bäuml, G., Bonaventura, L., Brokopf, R., Esch, M., Giorgetta, M., Hagemann, S., Kirchner, I., Kornbleuh, L., Manzini, E., Rhodin, A., Schlese, U., Schulzweida, U., and Tomkins, A.: The atmospheric general circulation model ECHAM5, Part 1: model description, Report No. 349, Max-Planck Institute for Meteorology, 127 pp., Hamburg, Germany, 2003.

Skamarock, W. C., Klemp, J. B., Dudhia, J., Gill, D. O., Barker, D. M., Duda, M., Huang, X.-Y., Wang, W., and Powers J. G.: A description of the Advanced Research WRF version 3, NCAR Tech Note NCAR/TN-475+STR, 125 pp., 2008.

Snyder, R. L.: Hand calculating degree days, Agr. Forest Meteorol., 35, 353–358, 1985.

Sütyemez, M.: Determination of pollen production and quality of some local and foreign walnut genotypes in Turkey, Turk. J. Agric. For., 31, 109–114, 2007.

Wallace, D. V., Dykewicz, M. S., Bernstein, D. I., Blessing-Moore, J., Cox, L., Khan, D. A., Lang, D. M., Nicklas, R. A., Oppenheimer, J., Portnoy, J. M., Randolph, C. C., Schuller, D., Spector, S. L., and Tilles, S. A.: The diagnosis and management of rhinitis: an updated practice parameter, J. Allergy Clin. Immun., 122, 1–84, 2008.

Warmund, M. R., Coggeshall, M. V., and Stamps, W. T.: Rest completion of eastern black walnut, J. Am. Pomol. Soc., 63, 64–71, 2009.

Zhang, R., Duhl, T., Salam, M. T., House, J. M., Flagan, R. C., Avol, E. L., Gilliland, F. D., Guenther, A., Chung, S. H., Lamb, B. K., and VanReken, T. M.: Development of a regional-scale pollen emission and transport modeling framework for investigating the impact of climate change on allergic airway disease, Biogeosciences Discuss., 10, 3977–4023, doi:10.5194/bgd-10-3977-2013, 2013a.

Zhang, Y., Qian, Y., Dulière, V., Salathé Jr., E. P., and Leung, L. R.: ENSO anomalies over the Western United States: present and future patterns in regional climate model simulations, Clim. Change, 110, 315–346, doi:10.1007/s10584-011-0088-7, 2012.

Zhang, Y., Isukapalli, S. S., Bielory, L., and Georgopoulos, P. G.: Bayesian analysis of climate change effects on observed and projected airborne levels of birch pollen, Atmos. Environ., 68, 64–73, doi:10.1016/j.atmosenv.2012.11.028, 2013b.

GMDD
6, 2325–2368, 2013

Table 1. Allergenic species/species groups and associated plant-functional type (PFT) classes included in initial simulations of the STaMPS model, as well as base temperatures (T_B) and GDD thresholds used to determine the timing of pollen release for each species/species group. "Var." stands for variable T_B, assigned to species such as oaks that exhibit geographic plasticity with respect to thermal requirements for blooming (T_B range in 12 km domain is ~ 0–8.7 °C).

Genus/species name (common name)	PFT class	T_B (°C)	GDD threshold
Quercus spp. early-blooming oak species (*Q. agrifolia, Q. lobata, Q. douglasii, Q. dumosa, Q. engelmannii, Q. laurifolia, Q. turbinella, Q. velutina, Q. virginiana, Q. wislizeni*) late-blooming oak species (*Q. alba, Q. chrysolepis, Q. coccinea, Q. gambelii, Q. garryana, Q. grisea, Q. Ilex, Q. kelloggii, Q. macrocarpa, Q. palustris, Q. rubra,* other *Q.* spp.)	trees (some are shrubs)	var.	*If $T_B < 7.3$, threshold = $(-150.78 \cdot T_B) + 1129$, accumulation begins 1 Feb; if $T_B \geq 7.3$, threshold = $(-29.179 \cdot T_B) + 540$, accumulation begins 1 Jan *GDD = $(-101.19 \cdot T_B) + 1515$, accumulation begins 1 Feb
Betula spp. (birch species), e.g. *B. pendula*	trees	9.1	620
Olea europaea (European olive)	trees	9.1	490
Platanus spp. (sycamore species) e.g. *P. acerifolia*	trees	var.	400
Morus spp. (mulberry species)	trees	var.	500
Juglans spp. (walnut species) including *J. regia* and *J. Californica*	trees	9.1	590
Bromus spp. (brome grasses) including *B. diandrus* and *B. mollis*	native grasses	15	See Table 2.

* Relationships between GDD thresholds and T_B for oaks are based on García-Mozo et al. (2002) and were modified to fit the oak species found in the model domain using observational data including pollen counts and oak phonological observations as described in Sect. 2.1.1.

GMDD
6, 2325–2368, 2013

Table 2. Relationship between chilling and GDD thresholds for brome grasses (derived from Gleichsner and Appleby, 1996).

No. of days (n) temp. $\leq 7\,^{\circ}$C	GDD to flowering, as a function of n
0	185
$0 < n \leq 42$	$0.080357 \cdot n^2 - 6.275 \cdot n + 183.4$
$42 < n$	59.5

GMDD
6, 2325–2368, 2013

Table 3. Land cover classes (as determined using the NASS CDL), associated STaMPS PFT classes and data sources used to assign species composition and fractional vegetation cover associated with each land cover classes.

Land cover class (based on CDL)	PFT class(es) represented	Source of species composition data	Source of fractional vegetation cover data
Forest	Trees	FIA[b]	NLCD[e] canopy
Urban	Trees	Urban tree inventories	Duhl et al. (2012)
Shrubland	Shrubby trees, shrubs[a]	NRCS[c]	NLCD canopy
Grassland herbaceous/ Open space	Grasses	NRCS	NLCD canopy, NLCD impervious
Agricultural[a]	Trees, grasses[a]	NASS CDL[d]	NLCD canopy

[a] Modules simulating pollen release from shrubs and agricultural grass species are under development.
[b] Forest Inventory and Analysis data (FIA, http://www.fia.fs.fed.us/).
[c] Natural Resource Conservation Service (soildatamart.nrcs.usda.gov/).
[d] National Agriculture Statistics Service Cropland Data Layer (NASS CDL, http://www.nass.usda.gov/research/Cropland/SARS1a.htm).
[e] National Land Cover Data (NLCD, http://www.mrlc.gov/index.php).

GMDD
6, 2325–2368, 2013

Table 4. Percent tree and non-tree cover assigned to urban CDL classes (based on Long Beach, CA).

CDL code	CDL land use class name	% tree cover	% non tree cover
122	Developed/Low Intensity	15	15
123	Developed/Medium Intensity	10	10
124	Developed/High Intensity	5	0.1

GMDD
6, 2325–2368, 2013

Table 5. Differences in domain-wide pollen production ("pollen %", in percent relative to current simulations) and average differences (avg. diff) as well as standard deviations (σ) in pollen season start dates (relative to current scenario), in days. *P* values and degrees of freedom (d.f.) are also shown for paired, two-sample *t* tests.

	Pollen production differences (as percentage relative to current scenario)			Average differences in start dates, FUTURE-CURRENT (in days)			
Genus	pollen %	*p* value	d.f.	avg. diff	σ	*p* value	d.f.
Betula	−3.32	$< 2.2 \times 10^{-16}$	1151	−5.6	3.4	$< 2.2 \times 10^{-16}$	1151
Bromus	−0.04	$< 2.2 \times 10^{-16}$	2483	−5.4	4.1	$< 2.2 \times 10^{-16}$	2483
early_oak	−6.77	$< 2.2 \times 10^{-16}$	3541	−4.9	2.0	$< 2.2 \times 10^{-16}$	3541
Juglans	0.01	$< 2.2 \times 10^{-16}$	1233	−6.0	3.0	$< 2.2 \times 10^{-16}$	1233
late_oak	9.03	$< 2.2 \times 10^{-16}$	2151	−5.5	1.1	$< 2.2 \times 10^{-16}$	2151
Morus	0.25	$< 2.2 \times 10^{-16}$	2143	−6.4	1.7	$< 2.2 \times 10^{-16}$	2143
Olea	−4.11	$< 2.2 \times 10^{-16}$	1283	−5.8	3.7	$< 2.2 \times 10^{-16}$	1283
Platanus	−1.21	$< 2.2 \times 10^{-16}$	2131	−6.2	2.1	$< 2.2 \times 10^{-16}$	2131
all species	**−3.36**	$\mathbf{< 2.2 \times 10^{-16}}$	**16 123**	**−5.6**	2.7	$\mathbf{< 2.2 \times 10^{-16}}$	16 123

GMDD
6, 2325–2368, 2013

Table 6. Number of domain cells (No. Cells) containing each genus selected for simulation, percent of cells meeting thermal and (for tree species with vernalization requirements) chilling requirements, and percentage flowering during the March–June simulation period.

Genus	No. Cells	% chill requirement met		% heat requirement met		total % flowering	
		CURRENT	FUTURE	CURRENT	FUTURE	CURRENT	FUTURE
Betula	2189	88.8	92.3	53.6	57.2	50.5	51.9
Bromus	3166	n/a	n/a	78.5	89.2	78.5	89.2
early_oak	4416	n/a	n/a	80.2	88.0	80.2	88.0
Juglans	2146	98.7	99.5	57.6	60.5	57.6	60.5
late_oak	4108	n/a	n/a	52.4	57.8	52.4	57.8
Morus	2218	n/a	n/a	96.7	99.2	96.7	99.2
Olea	2142	88. 6	92.1	60.9	63.4	57.8	57. 9
Platanus	2142	n/a	n/a	99.5	99.9	99.5	99.9

GMDD
6, 2325–2368, 2013

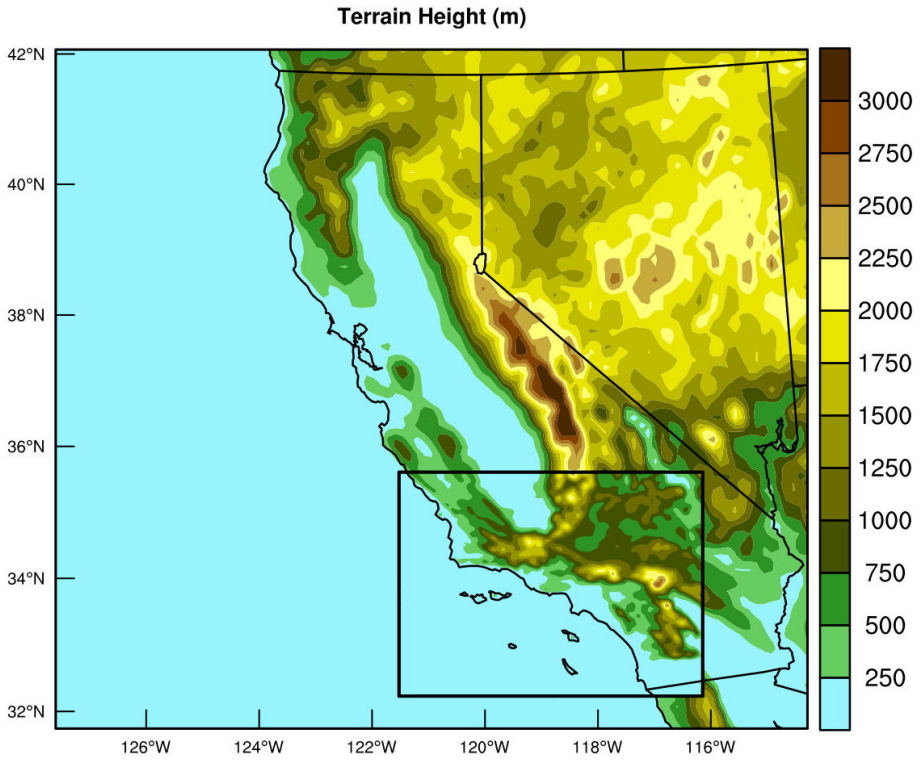

Fig. 1. Extent of the 12 km model domain used for the current and future simulations and smaller 4 km domain (small box centered over S. California) used to evaluate simulation results for the year 2010 as described in Zhang et al. (2013a). Surface elevations are color-coded to show elevation in m.

GMDD
6, 2325–2368, 2013

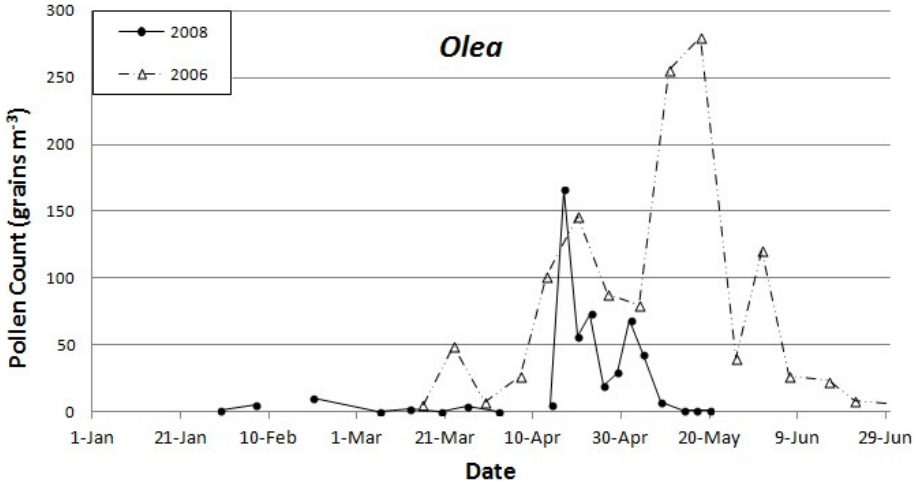

Fig. 2. Olive tree pollen counts data for Pasadena, CA, 2006 and 2008.

GMDD
6, 2325–2368, 2013

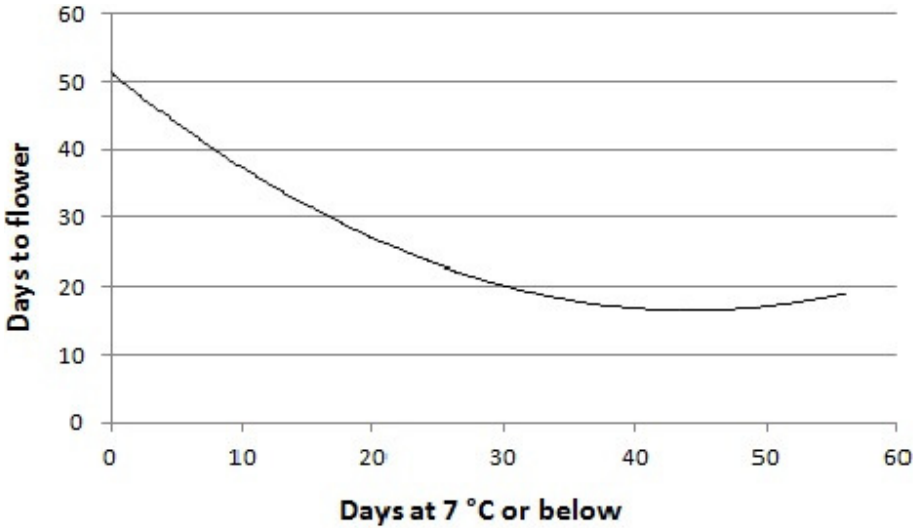

Fig. 3. Effect of exposure to cold temperatures on flowering time in *Bromus diandrus* (derived from Gleichsner and Appleby, 1996).

GMDD
6, 2325–2368, 2013

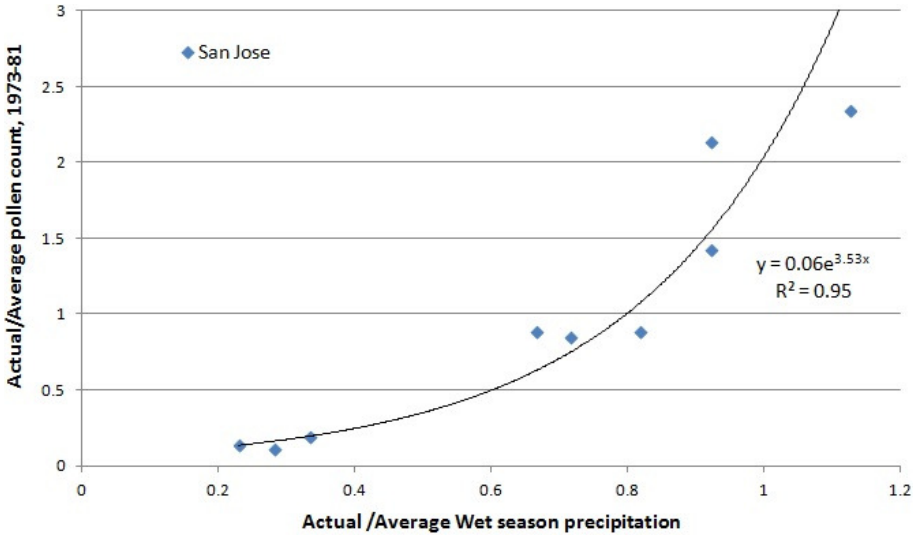

Fig. 4. Relationship between wet season precipitation and pollen production as modeled for tree species in the domain (derived from Fairley and Batchelder, 1986).

GMDD
6, 2325–2368, 2013

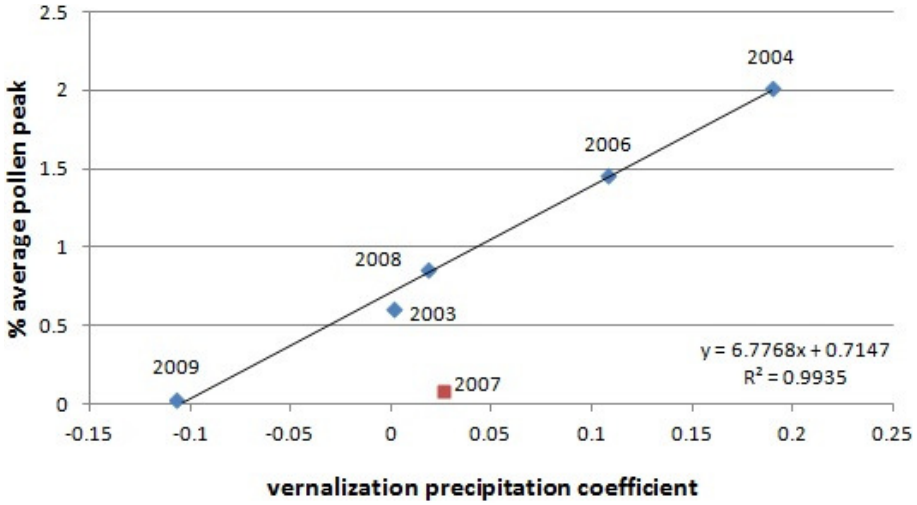

Fig. 5. Relationship between pollen production (expressed as percent of average peak value) and dual vernalization-precipitation coefficient (as calculated using Eq. 6) derived from Pasadena CA data and applied to STaMPS tree species with quantitative vernalization requirements for flowering.

GMDD
6, 2325–2368, 2013

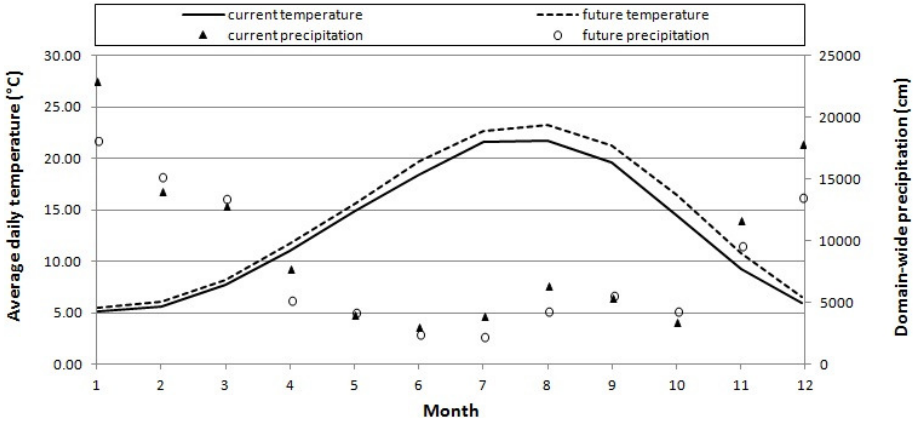

Fig. 6. Domain-wide average monthly precipitation and temperature for current and future simulations.

GMDD
6, 2325–2368, 2013